Electronic Supplementary Material (ESI) for Environmental Science: Nano.

Supplemental information

Two-stage hierarchical clustering for analysis and classification of mineral sunscreen and naturally occurring nanoparticles in river water using single-particle ICP-TOFMS

Hark Karkee and Alexander Gundlach-Graham*

Department of Chemistry, Iowa State University, Ames, Iowa

Address correspondence: alexgg@iastate.edu

Table of Contents

Table S1: Dilution scheme for the spiking of sunscreen particles into river water. Results for quantification of SS particles are provided in Figure 5.

Quantification of spiked sunscreen in 50X diluted river water			
		ENP PNCs in stock (Particles per mL^{-1}) 1.00E+06	
Sample no.	Volume of river water (µL)	Volume of Sunscreen stock suspension (diluted in 5 ng mL^{-1}Cs water) (µL)	Volume of DI water containing 5 ng mL^{-1} Cs (µL)
S1	200	10	9790
S2	200	50	9750
S3	200	250	9550
S4	200	500	9300
S5	200	2500	7300
S6	200	5000	4800

Table S2: Dilution scheme for the spiking of sunscreen particles in river water with added Ti-minerals (biotite, ilmenite and rutile). Results for quantification of SS particles are provided in Figure S5.

Quantification of spiked sunscreen in 50X diluted river water containing added Ti-minerals				
		ENP PNCs in stock (Particles per mL^{-1}) 1.00E+06	NNP PNCs in stock (Particles per mL^{-1}) 1.00E+05	
Sample no.	Volume of river water (µL)	Volume of Sunscreen stock suspension (diluted in 5 ng mL^{-1} Cs water) (µL)	Volume of NNP stock suspension (diluted in 5 ng mL^{-1} Cs water) (µL)	Volume of DI water containing 5 ng mL^{-1} Cs (µL)
S1	200	10	1000	8790
S2	200	50	1000	8750
S3	200	100	1000	8700
S4	200	250	1000	8550
S5	200	500	1000	8300
S6	200	2500	1000	6300
S7	200	5000	1000	3800

Table S3: Concentrations of elements in online microdroplet calibration solution. Typical sensitivity and critical mass values obtained with spICP-TOFMS analysis.

Element Name	Isotopes Used	Sensitivity (Tofcts/g)	$X^{mass}_{C,sp}$ (g)	Concentration in droplets (ng mL^{-1})
Mg	^{24}Mg	2.23E+16	2.37E-15	25.3
Al	^{27}Al	2.01E+16	3.80E-16	25.6
Ti	^{46}Ti or ^{48}Ti	1.12E+17	1.71E-16	25.8
V	^{51}V	1.76E+17	8.54E-17	25.6
Mn	^{55}Mn	1.63E+17	8.31E-17	25.5
Fe	^{56}Fe	1.85E+17	8.61E-17	25.4
Co	^{59}Co	2.43E+17	4.29E-17	25.5
Zn	^{66}Zn	2.16E+16	5.26E-16	25.5
Y	^{89}Y	2.04E+17	3.83E-17	25.4
Zr	^{90}Zr	1.73E+17	3.98E-17	25.6
Nb	^{93}Nb	3.04E+17	2.23E-17	25.6
Cs	^{133}Cs	2.16E+17	NA	25.3
La	^{139}La	4.65E+17	1.19E-17	25.5
Nd	^{146}Nd	4.90E+16	1.13E-16	25.3
Ce	^{140}Ce	4.26E+17	1.42E-17	25.5
Ta	^{181}Ta	3.49E+17	1.49E-17	25.5
W	^{182}W	1.29E+17	3.89E-17	25.7
Pb	^{206}Pb, ^{207}Pb and ^{208}Pb	2.36E+17	4.17E-17	25.4

Table S4: Instrument parameters

Online Microdroplet Parameters	
Droplet Size	69.93 µm
Falling tube gas (Ar)	19 mL min^{-1}
Falling tube gas (He)	360 mL min^{-1}
ICP Parameters	
Spray Chamber	Baffled cyclonic quartz
Nebulizer	PFA PrepFAST
Nebulizer gas	0.79 L min^{-1}
Auxillary gas	1.13 L min^{-1}
Cool gas	14.5 L min^{-1}
RF power	1500 W
Sampling depth	4.42 mm
Mass Spectrometer Parameters	
Extraction Lens	-203 V
CCT mass	222 V
CCT Bias	-4.0 V
CCT H2 flow rate	6 mL min^{-1}
Notch filter (m/z)	17.3, 31, 37, 38.2
Average spectrum acquisition rate	838 Hz
Time resolution	1.19 ms
Number mass spectra averaged per time point	99

Table S5: Element and sample-specific critical masses for spICP-TOFMS analyses of neat suspensions of SS and RW (see Fig. 1)

	Critical Masses (ag)	
Element	**SS (neat)**	**RW (neat)**
Mg	245	2695
Al	140	288
Ti	42	212
V	164	164
Mn	38	64
Fe	77	97
Co	31	35
Cu	105	144
Zn	319	731
Y	22	35
Zr	32	43
Nb	18	29
La	9	14
Nd	86	99
Ce	8	15
Ta	18	44
W	32	46
Pb	26	32

Table S6: Element and sample-specific critical masses (ag) for spICP-TOFMS analyses of neat suspensions of SS and RW and mixed samples (S1-S6) used for HCA analysis (see Fig. 3) and quantification of SS particles in RW samples (see Fig. 5)

	Sample-specific Critical Masses (ag)							
Element	**SS**	**RW**	**S1**	**S2**	**S3**	**S4**	**S5**	**S6**
Mg	705	2366	2150	2186	1936	2095	2012	2014
Al	482	380	429	277	242	298	275	271
Ti	72	171	170	172	165	169	156	145
V	159	85	85	79	79	79	75	74
Mn	83	83	75	60	73	82	80	81
Fe	203	86	98	121	98	100	156	129
Co	40	43	40	30	31	36	38	34
Cu	247	169	159	135	192	194	164	178
Zn	919	526	566	520	569	575	928	784
Y	33	38	38	39	41	42	41	39
Zr	40	40	42	40	41	44	43	44
Nb	17	22	23	22	25	26	25	23
La	16	12	13	13	14	13	18	14
Nd	106	113	110	111	116	116	116	116
Ce	33	14	19	17	16	16	32	21
Ta	15	15	15	15	16	16	16	16
W	37	39	41	41	42	42	42	42
Pb	52	42	34	30	29	31	30	31

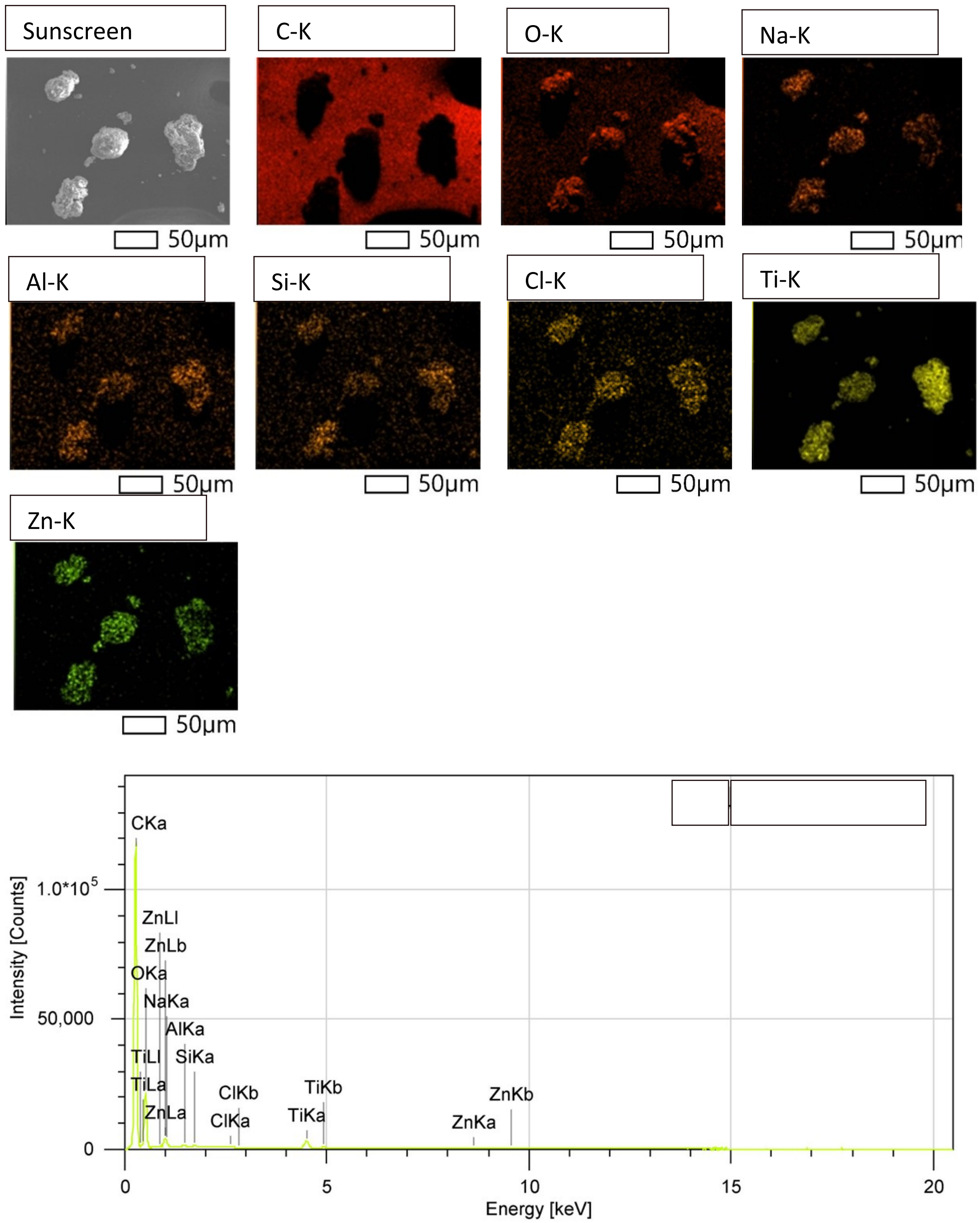

Figure S1: SEM images and EDS spectrum of sunscreen particles

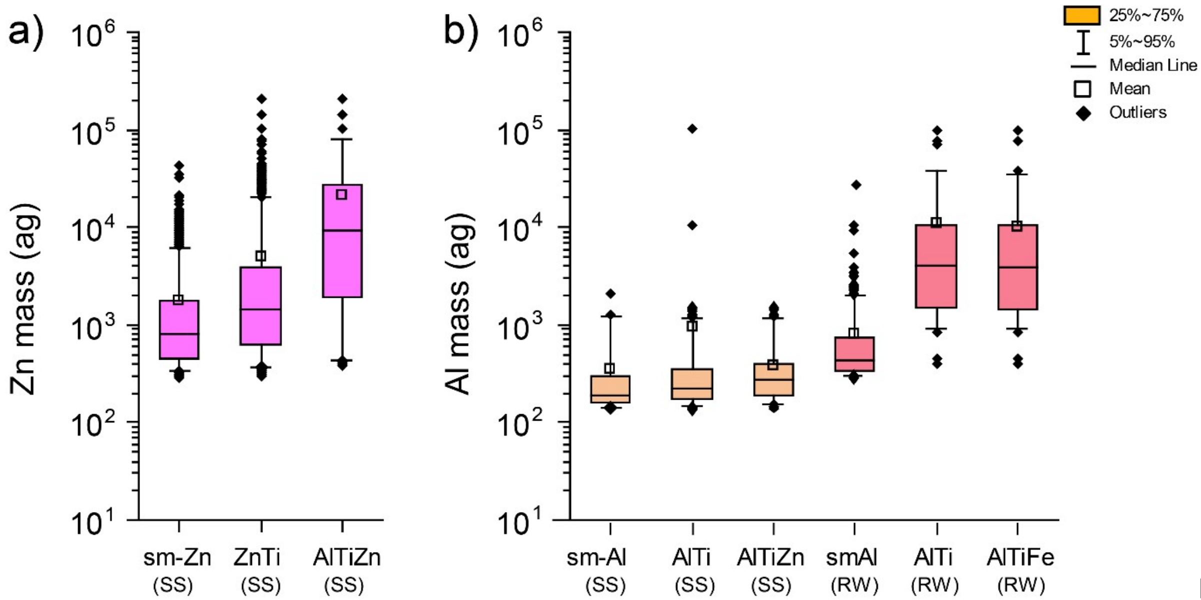

Figure S2: **a)** Boxplots showing mass distribution of Zn in particles measured with differing elemental signatures in sunscreen (SS). **b)** Mass distribution of Al in sunscreen and river water (RW) particles.

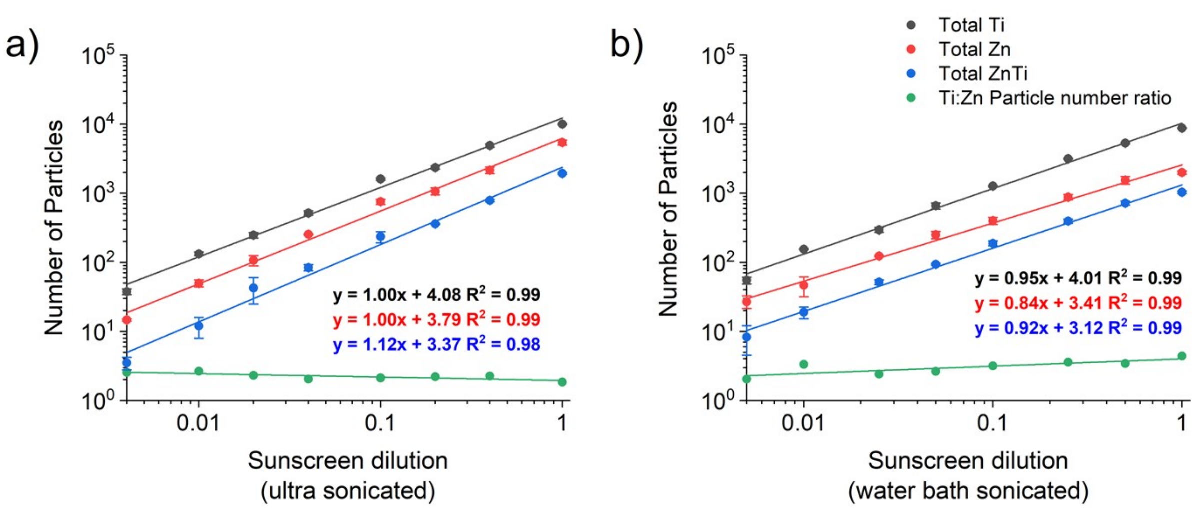

Figure S3: Numbers of Ti, Zn, and ZnTi particles measured by spICP-TOFMS after particles from the neat sunscreen suspension were extracted using ultrasonication (a) and water bath sonication (b). Linear response of all measured particle types indicates TiZn aggregates are real signals and are not loosely bound.

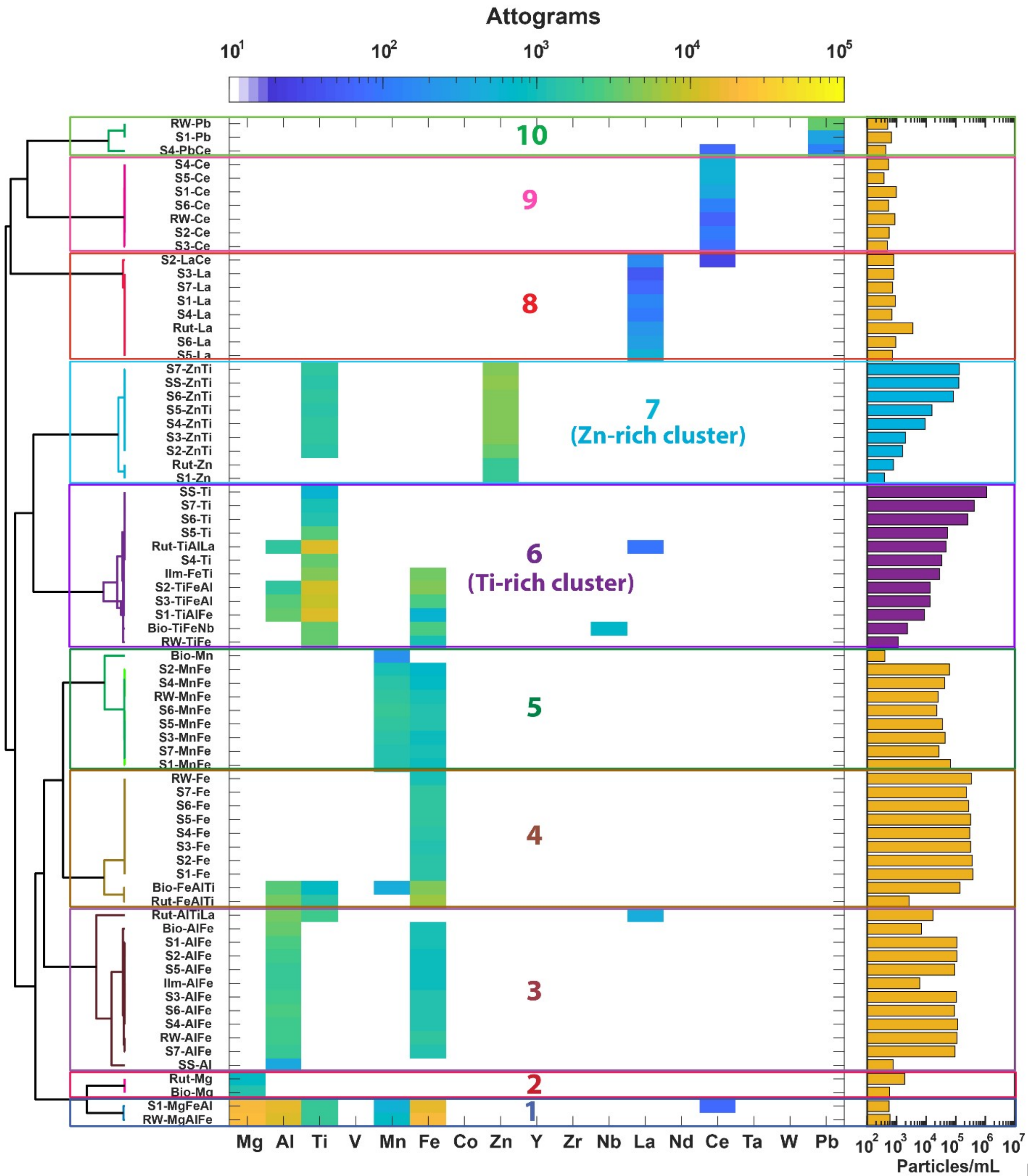

Figure S4: Dendrogram from two-stage unsupervised hierarchical clustering analysis (HCA) of SS + RW + Ti-mineral samples. The heat map indicates the occurrence-normalized mean mass of each element in the found particle-class proxy (PCP) from the 1st-stage (intra-sample) clustering and the PNCs (particles mL^{-1}) of each PNC are provided as bars on the right.

Results from two-stage HCA where sunscreen particles are spiked in RW with enriched Ti-minerals (rutile, ilmenite and biotite) are provided in Figure S4. Particle-class proxies (PCPs) from 1st stage of HCA are grouped into a total of ten major clusters, numbered 1-10. Each of the PCP is identified as the name of sample (SS-sunscreen, RW-river water, rut-rutile, ilm-ilmenite, bio-biotite and S1-S7 for mixtures of RW, Ti- nanominerals and SS with increasing concentrations of SS particles). Like what we observed in Figure 3, SS-derived clusters (Ti-rich and Zn-rich clusters) are distinct from the RW + Ti- nanominerals derived clusters (clusters 1, 2, 3, 4, 5, 8, 9 and 10); however, the Ti-rich cluster is more influenced by Ti-particles from the Ti- nanominerals. PCPs originating from RW (RW-TiFe) and added Ti- nanominerals (Bio-TiFeNb, Ilm-FeTi and Rut-TiAlLa) are also clustered along with the SS PCP (SS-Ti). In the Ti-rich cluster, the most dilute samples (S1, S2 and S3) show elevated PNCs due to Ti-particles from RW and Ti-nanominerals. On the other hand, the Zn-rich cluster does not contain RW particles, and is minimally influenced by added rutile Zn-particles. Such Zn-rich particles from rutile are unlikely to be present in environmental samples such a river water or soil unless the sampling site is rich in rutile mineral or a Zn-bearing mineral.

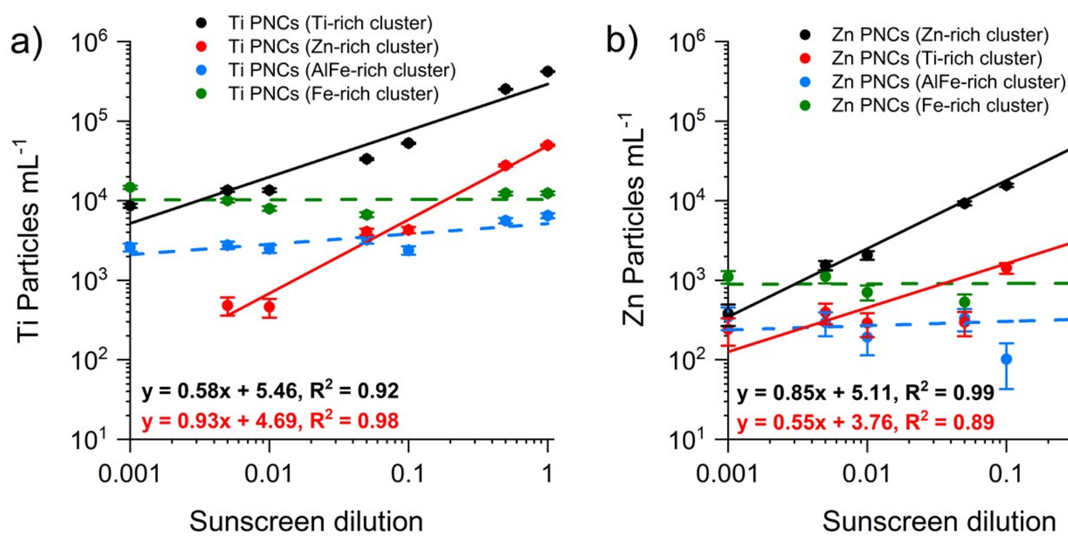

Figure S5: Quantification of Ti-bearing NPs **(a)** and Zn-bearing NPs **(b)** spiked from sunscreen into river water enriched Ti-nanominerals. Data points plotted are based on particles mL^{-1} present in merged (triplicate measurements merged for HCA) data files. Error bars plotted are the predicted standard deviation based on Poisson-Normal statistics.

As we discussed earlier, the Ti-rich and Zn-rich clusters are considered to be characteristic of SS and, the AlFe-rich and Fe-rich clusters are considered to be characteristic of RW. Figure S4 shows the results of two-stage HCA of neat and mixed samples (mixture of SS, RW and Ti-nanominerals). In Figure S5, we present quantification of the SS particles spiked in RW enriched with Ti-nanominerals. Ti and Zn particles present in spiked samples S1-S7 were extracted from SS derived clusters (Ti-rich and Zn-rich). Additionally, Ti and Zn particles were also extracted from RW enriched with Ti-nanominerals clusters, specifically cluster 3 (AlFe-rich cluster) and cluster 4 (Fe-rich cluster. These clusters can be seen in Figure S4. SS derived Ti PNCs and Zn PNCs are plotted in Fig. S5a and Fig. S5b, respectively, against the Ti and Zn PNCs derived from RW enriched with Ti-nanominerals. On a log-log plot, a slope of 1 indicate linear response. The slope of Ti-PNCs in Fig. S5a is significantly lower than 1 and also lower than the slope of Ti-PNCs spiked in RW without enriched Ti-nanominerals (see Fig. 5a). The non-linearity of the Ti PNCs in the Ti-rich cluster is due to influence Ti-particles from added Ti-nanominerals. On the other hand, for Ti-containing particles in the Zn-rich cluster, the PNC vs. dilution amount has slope of 0.93, which indicating that Ti-particles in Zn-rich cluster could be a reliable measure to classify the SS particles. We also find linear increment of Zn particles in Zn-rich cluster with increase in the concentration of SS. The slope is less than 1 due presence of small number of Zn particles in RW water which artificially increases the PNCs of Zn, as compared to the expected Zn PNCs from SS, especially in samples with the most dilute SS particle suspensions.